Title
Under what conditions does land cover change impact regional climate

Authors
Xue, Y
Fennessy, M

Publication Date
2002

Peer reviewed

4

Under What Conditions Does Land-cover Change Impact Regional Climate?

Y. XUE[1] and M.J. FENNESSY[2]

[1]Department of Geography, University of California, Los Angeles, CA 90095–1524, U.S.A.
[2]Center for Ocean-Land-Atmosphere Studies, Calverton, MD 20705–3106, U.S.A.

ABSTRACT

This chapter reviews studies that have investigated the impact on regional climate of land degradation caused by land-cover changes in the Sahel, East Asia, and the central United States. Numerical experiments with coupled general circulation model/biosphere models show that land degradation led to a reduction in rainfall, evapotranspiration, soil moisture, and runoff, as well as an increase in surface temperature and near-surface wind field. In Sahel and East Asian studies, a coupled model produced anomaly patterns consistent with the long-term droughts observed. In the Sahel, the simulated climate anomaly is not limited to the specified degradation area and the summer rainy season but extends to the south and into the autumn. In the East Asian simulation, the degradation of the Mongolian and Inner Mongolian grasslands produces a rainfall anomaly extending far to the south of the degraded area. In the central U.S., the regional climate is also very sensitive to the surface vegetation conditions; however, the simulated anomalies are primarily limited to within the area where the land conditions are changed. In all these experiments, changes in the hydrological cycle were the most important in producing the climate anomalies, in contrast to the conventional view that radiative effects dominate.

INTRODUCTION

The relationship between changes in land cover and climate variations has long been a subject for scientific research (Goudie 2000). Although much observational evidence supports the idea that such a link exists, quantitative measures of it were unavailable until more sophisticated models were developed during the 1980s. In this chapter, we present results from

Global Desertification: Do Humans Cause Deserts?
Edited by J.F. Reynolds and D.M. Stafford Smith
ISBN 3-934504-10-8 To order book, contact: dahlemup@zedat.fu-berlin.de

coupled atmospheric and land-surface models to demonstrate how land-cover change affects several regional climates.

Two regions of the world, the Sahel and East Asia, experienced significant droughts during the 1980s (Figure 4.1), and desertification has been considered as one of the causes. Figure 4.1 is based on Hulme's climate data (Hulme 1992). The Sahel is a strip of semi-arid land (approximately 1.5 million km^2) bordering the southern edge of the Sahara. Today it is a bioclimatic zone of predominantly annual grasses with shrubs and trees, receiving a mean annual rainfall of between 150 and 600 mm per year. Since the late 1960s, a persistent drought has lasted for more than 30 years. Although in the 1990s rainfall was not as scarce as in the 1980s, it was still below the climatological average. One of the important features of sub-Sahara drought is the southward displacement of the intertropical convergence zone (ITCZ) in the northern Sahel during the dry years. This redistribution reduces the rainfall in the Sahel while increasing it to the south of 10°N (Figure 4.1). Although the maximum rainfall was not reduced very much, the shift resulted in the rainfall deficiency in the Sahel (Xue and Shukla 1993).

Observations in mainland China from 1951 to 1990 also reveal that, in general, the climate has been drying since the 1950s (Xue 1996; Yatagai and Yasunari 1995). Both southern and northern China became increasingly dry from the 1950s to the 1980s, but rainfall increased in the Yangtze River region. Thus, the rainfall anomaly has a negative-positive-negative (N-P-N) pattern (Figure 4.1).

The rainfall reductions in the Sahel and China mainly occur during June, July, and August, and are related to variations in the African and East Asian summer monsoons. It is possible that persistent droughts in recent years may be related to anthropogenic changes in land

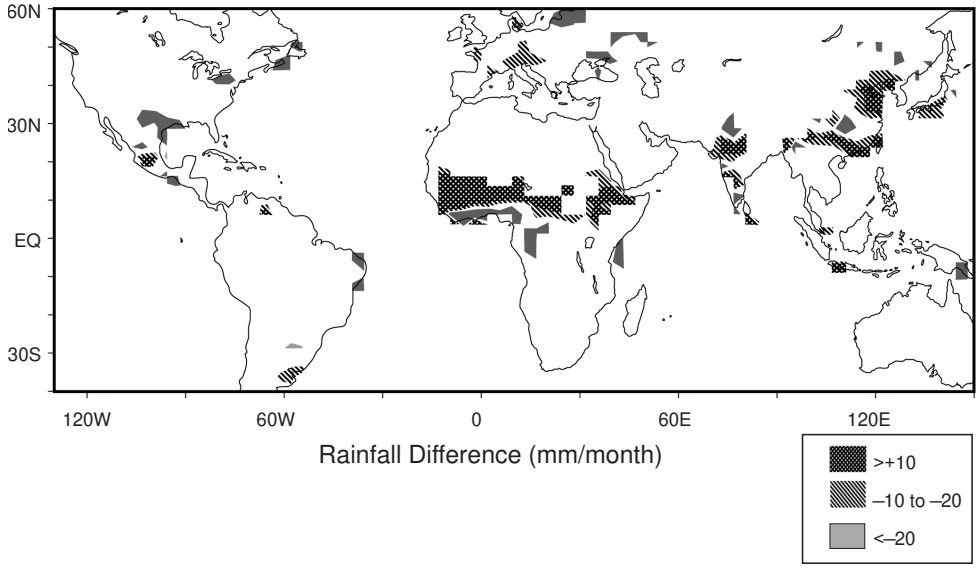

Figure 4.1 Observed June-July-August rainfall difference over land between the 1980s and 1950s (mm $month^{-1}$).

cover. The droughts in the Sahel and East Asia coincide with degradation of the land surface that has occurred in both areas during the past half century.

Rapid population growth has occurred in these regions over the past fifty years. The population of five Sahelian countries (Senegal, Niger, Mali, Sudan, and Chad), for example, rose from 20 million in 1950 to 55 million in 1990, and is projected to rise to over 135 million by 2025 (WRI 1994). This rise in population, as well as political constraints on nomadism, (Middleton 1999) could cause extensive land-cover conversion. The Sahelian region has undergone significant changes in land cover over the past decades. A number of studies have shown that overgrazing of the natural rangelands by livestock, agricultural expansion, agricultural intensification, and increased fuel-wood extraction, coupled with severe drought, are leading to widespread land degradation in the Sahel. Previously uncultivated areas experience agricultural expansion as a result of migration into unsettled areas, aided by newly developed technologies (Gornitz 1985; Dregne and Chou 1992; Middleton 1999; Goudie 2000; Stephenne and Lambin 2001; Xue et al. 2003).

Some have challenged this view of the large-scale land degradation (Nicholson et al. 1998; Nicholson 2002), based primarily on satellite data from the late 1970s. However, we believe that measuring rates of dryland degradation is a complex challenge to remote sensing technology and retrieval methodology, requiring a long time series of rainfall data, remote sensing-based indicators of surface conditions, field observations of soil attributes, floristic composition, etc. to produce reliable results.

In northern China, there are vast areas of desertification-prone land (about 334,000 km^2), of which about 176,000 km^2 is already desertified (Zhu et al. 1988). The desertified area expanded at a rate of 1,560 km^2 per year from the 1950s to the 1970s. A large part of this area is located in the Inner Mongolian grassland. Desertification there can be classified into three types: desertification of sandy steppe, the reactivation of fixed dunes, and the encroachment of sand dunes. The desertified areas are adjacent to regions of mixed pasture and agricultural land use, where the ecosystem is especially vulnerable to external forcing (both natural and anthropogenic). The Inner Mongolian grassland is the main pasture region in China. Rapidly expanding population, increasing human land use, and agricultural development have led to environmental degradation. Over-cultivation on the steppe, overgrazing, and wood gathering were responsible for 25%, 28%, and 32% of the total desertified area from the 1950s through the 1980s, respectively (Zhu et al. 1988). Thus, the increase in human activities accelerated desertification in the 1980s. Several large regions (such as Ulanqab, North Hebei, Chahar) experienced almost a doubling of desertified areas in this time period.

The human tragedies and severe socioeconomic consequences resulting from drought-induced famines in the Sahel region provide strong motivation for research into the causes of the drought. Below, we review studies that explore the conditions under which land-surface changes can cause changes in the regional climate.

SAHEL DESERTIFICATION STUDY

It has long been conjectured that changes in land-surface properties affect the energy and water balance, and may be responsible for alteration of the regional climate. However, the hypothesis proposed by Charney (1975) — that there is a positive feedback between northern African drought and land-surface albedo — is still unresolved. He used a simple model to

demonstrate that the high surface albedo associated with land degradation could cause radiative cooling of the atmosphere leading to sinking motion, which could lead to reduced rainfall in tropical Africa. Charney's hypothesis and demonstration that land-surface changes could cause regional climate anomalies were challenged because (a) the magnitude of the albedo change in his simulations was not supported by observations and (b) the surface temperature cooling due to high albedo was contrary to common sense, that high surface temperature was normally associated with the desertification (see Nicholson 2002). Analyzing satellite observations, Norton et al. (1979) found that the albedo in West Africa increased during the period 1967 to 1973. During the wet seasons, the albedo changed from 0.23 in 1969 to 0.33 in 1973. This discovery was also confirmed by a recent study (Nicholson et al. 1998). The range of variation of 0.1 in these studies is far less than the dramatic changes that were made in Charney's study. Charney later realized that changes in evaporation might be as important as albedo changes (Charney et al. 1977).

During the 1980s, a number of studies with different general circulation models (GCMs) were conducted to examine the role of land-cover changes in regional climate. In these studies the parameterizations of surface processes were very simple. Some models had no soil moisture, while others used a bucket-type model, which likened the land surface to a bucket of water. In this oversimplified model, a portion of the water in a bucket evaporated into the atmosphere based on empirical equations.

As a result of limitations in model development and in understanding of land-surface interactions during the later 1970s and 1980s, Sahelian modeling studies were mainly boundary perturbation sensitivity studies. The area and magnitude of modeled land-surface changes, such as albedo and soil moisture, were very dramatic. The idea was that if such large changes in the models were unable to produce substantial variations in the simulated regional climate, further research in this direction would be in vain.

In a GCM, Charney et al. (1977) found that increases in albedo caused a reduction in precipitation in semi-arid regions. This discovery was confirmed by a number of studies with different models (e.g., Chervin and Schneider 1976; Sud and Fennessy 1982; Laval and Picon 1986). The effects of soil moisture and evaporation have also been investigated (e.g., Walker and Rowntree 1977; Sud and Fennessy 1984). Most of these studies showed that less initial soil moisture leads to less precipitation. Furthermore, the combined effects of surface albedo and soil moisture were studied (e.g., Sud and Molod 1988; Kitoh et al. 1988). Kitoh et al. found that the combined effects almost equalled the sum of the albedo and soil moisture effects alone. The role of other factors, such as atmospheric water content and radiation schemes in land–atmosphere interactions, have also been investigated (Cunnington and Rowntree 1986). These modeling studies consistently demonstrated that the land surface might have a significant impact on the Sahel climate. They also generated public and government support for further research in this direction, despite the simplicity in experimental design and model parameterizations.

Atmosphere–biosphere interactions are much more complex in the real world and involve many more parameters and processes. Therefore, sophisticated land-surface models are needed to assess the impact of desertification on the Sahel drought realistically. A proper evaluation of the surface feedback on climate can be obtained only when all components of the energy and water balances are considered. Starting from the mid-1980s, a number of surface schemes, including a realistic representation of the vegetation responses, have been

applied to the Sahel (e.g., the biosphere–atmosphere transfer scheme, BATS [Dickinson et al. 1986] and the simplified simple biosphere model, SSIB [Xue et al. 1991]). These schemes have been coupled with atmospheric models to conduct a number of Sahel drought studies (Xue et al. 1990; Xue and Shukla 1993; Xue 1997; Clark et al. 2001). More realistic surface models and more realistic changes in land-surface conditions should help improve our understanding of the mechanisms of land–atmosphere interactions.

Here we present the results from the Center for Ocean–Land–Atmosphere Studies (COLA) GCM (Kinter et al. 1988) coupled with the SSIB (Xue et al. 1991). For the numerical simulations, a one-degree resolution world vegetation map aggregated to the GCM grid provides the land-surface conditions (for details, see Xue et al. 1996). Twelve vegetation types are recognized by SSIB, including trees, short vegetation, arable crops, and desert. Different vegetation and soil properties, including surface albedo, leaf area index (LAI), green-leaf fraction, surface roughness length, soil hydraulic conductivity, and the parameters that control aerodynamic resistances and stomatal resistance, are defined for each vegetation type. For the land-surface degradation simulations, savanna (Type 6) and shrubs with ground cover (Type 8) in the specified degradation area were changed to the shrubs with bare soil (Type 9), altering the prescribed vegetation and soil properties to that consistent with land degradation (Table 4.1). The degradation areas were chosen based on the world desertification map (UNEP 1992), which was the only source available describing global-scale land degradation at that time. This map, however, may not accurately represent desertification over the world (see, e.g., Nicholson 2002). Accurate, quantitative measurements of land degradation are crucial to understand and further investigate this problem.

To explore the impact of land degradation in the Sahel on seasonal climate variations and the soil hydrology, the coupled model has been integrated with different vegetation maps. As

Table 4.1 Vegetation parameters for five vegetation types.

	Type 6 (savanna)	**Type 7** (grassland)	**Type 8** (shrubs with ground cover)	**Type 9** (shrubs with bare soil)	**Type 11** (bare soil)
Mean surface albedo	0.20	0.23	0.20	0.28	0.32
Roughness length* (m)	0.95	0.08	0.25	0.06	0.01
Leaf area index (LAI)*	4.12	3.80	0.86	0.31	0
Greenness*	0.81	0.70	0.70	0.71	0
Minimum stomatal resistance (s/m)	282	117	1049	1049	
Vegetation cover	0.3	0.9	0.1	0.1	0
Total depth of three soil layers (m)	3.5	1.5	1.5	1.5	0.49
Hydraulic conductivity of saturated soil (m/s)	0.2E–4	0.2E–4	0.176E–3	0.176E–3	0.176E–3
VSMC at the wilting level**	0.13	0.13	0.05	0.04	

* The numbers are for the means of June, July, and August.
** VSMC is the volumetric soil moisture content.

a result of the internal variability inherent in GCM simulations, it is important to minimize the noise level when designing GCM experiments and to assess the significance of the results. The noise level may be reduced by time averaging over longer intervals and by increasing the sample size (see, e.g., Chervin and Schneider 1976). In Xue's study (1997), four-year simulations and three different initial atmospheric conditions were used to obtain results with more statistical confidence. Ensemble means of these simulations were used to detect the climate impact of the degraded land-surface conditions. The simulated anomalies were caused by both spatial and temporal changes in the land-surface conditions, and no attempt was made to test their impact separately.

Climatological sea-surface temperatures (SST) were used as the lower atmospheric boundary conditions over the oceans. For each initial condition, the model was integrated using the normal vegetation map (control simulation) and a degraded vegetation map (Figure 4.2), where savanna or shrubs with ground cover were changed to shrubs with bare soil in the degraded simulation.

The July-August-September mean (JAS) rainfall difference between the degraded and control simulations is shown in Figure 4.3. The rainfall is reduced in the degraded area, but increased slightly to the south. This dipole pattern is consistent with the observed pattern for dry climate anomalies (Figure 4.1). The rainfall changes are significant at the 90% confidence level in the area enclosed by dotted lines in Figure 4.3. The simulated rainfall in a test area (from 9°N to 17°N, and 15°W to 43°E), including most of the degraded area, is reduced by 39 mm month^{-1}, close to the 45 mm month^{-1} observed reduction. These results are consistent with previous short-term integrations (Xue and Sukla 1993), in which different SST

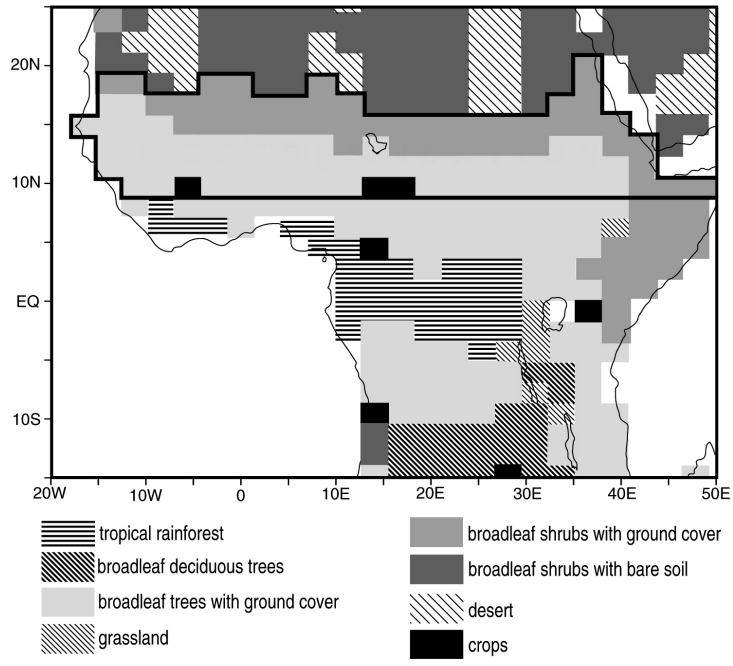

Figure 4.2 African vegetation classification map. Simulated degraded area is enclosed by heavy line.

boundary conditions were used. Figure 4.3 also reveals that the impact is not only limited to the Sahel, but also extends to some tropical regions. However, only over the Sahel and some of the tropical regions are the model results significant at the 90% confidence level.

At the beginning of the Sahelian dry season (October-November-December, OND), when the ITCZ moves to the south, little rainfall was observed or simulated in the Sahel. However, the simulated areas of reduced rainfall related to land degradation also shifted to the south of the Sahel, and there was a positive anomaly simulated over eastern Africa, consistent with the observed OND rainfall anomaly (not shown). Thus, the effect of the land degradation is not limited to the summer rainy season and is not limited to within the Sahel, but extends to the East Africa region during the autumn season.

The JAS surface air temperature was higher in the degraded simulation than the control, consistent with the observed JAS temperature difference between the 1980s and the 1950s. In the test area, the simulated surface air temperature increased by 0.8 K, close to the observed increase over the same area (1.1 K). The surface wind became stronger in the desertification area because of lower surface roughness, which would increase the wind erosion.

Soil moisture, surface runoff, and subsurface drainage in the degradation experiments decreased, consistent with the reduction in rainfall. The simulated river discharges from the control and degradation experiments at different stations were compared with the observed 1951–1970 and 1971–1990 means, respectively. The difference in the river discharge between the control and degraded simulations corresponded to the difference observed between 1951–1970 and 1971–1990 (Oki and Xue 1998). Due to the limitation in model grid sizes, only macro-hydrological processes were examined.

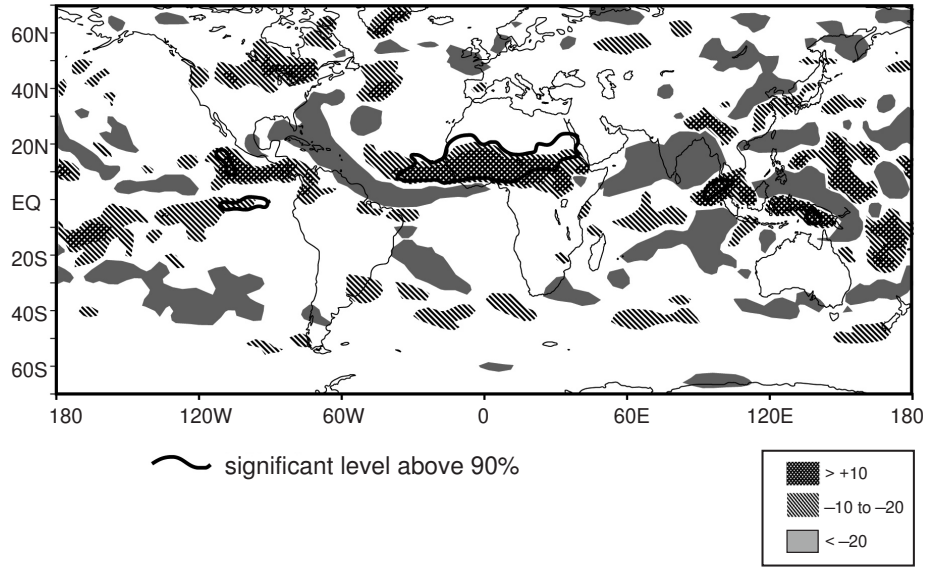

Figure 4.3 Difference in ensemble mean June-July-August (JJA) rainfall, degraded minus control simulation; Unit is mm month^{-1}. The results within the areas enclosed by solid and dash lines (with t-test number 1.44) have 90% statistic significance.

In the multiyear simulations, the simulated runoff anomalies changed signs after the first year. The reduced evaporation produced larger runoff during the first year. During the remaining years of the integrations, the total runoff was lowered by 9 mm month^{-1} over the southern Sahel, which is consistent with the reduction in precipitation. Thus, without the atmospheric feedback of reduced precipitation, land-surface degradation may produce more runoff as observed in small basins over short time scales.

Because of the lack of quantitative data to identify the extent and degree of Sahel desertification, we designed another set of experiments to investigate how the extent of the specified land-surface changes might affect the results. Five different subregions were degraded in turn: northern Sahel, southern Sahel, West Africa, East Africa, and the coastal area along the Gulf of Guinea (Clark et al. 2001). In general, the degradation resulted in reduced rainfall over the degraded area. However, considerable differences in the impact among the different areas indicated that the location and extent of the degradation area was important. The degradation in the northern Sahel and the West African Sahel resulted in the largest and most significant reductions of rainfall. In particular, degradation of the northern Sahel caused a widespread reduction in rainfall across tropical northern Africa, both within and outside the degraded area. Deforestation in the coastal area produced the least impact on the rainfall.

In the above numerical experiments, the vegetation types along with their vegetation and soil properties were changed. There are about twenty parameters in SSIB. We conducted another series of experiments, in which individual parameters or a set of vegetation parameters were changed in the degradation area. These experiments showed that among the parameters, the surface albedo, surface aerodynamic resistance, stomatal resistance, LAI, and hydraulic conductivity of the soil had the largest impacts on the simulations. The albedo changes used in Xue's (1997) Sahel study were reasonable (0.09–0.1) and close to the observed albedo difference between the cropland and natural vegetation in the Sahel (Nicholson et al. 1998). Despite the importance of albedo, changes in vegetation and soil properties (such as LAI) also contributed significantly to the simulated rainfall and surface temperature anomalies.

Land degradation also impacted the simulated large-scale circulation and easterly wave propagation. One of the important features of sub-Sahara drought is the displacement of the ITCZ in the dry years. Observations show that the maximum rainfall was not reduced very much in dry years (Xue and Shukla 1993). The shift in the observed rainfall gave rise to the rainfall deficiency in the Sahel. In the model simulations, both a shift and a reduction in the maximum rainfall played roles in reducing the rainfall in the Sahel. Both the strength and the depth of the monsoon flow in the simulation were changed (Xue and Shukla 1993).

Based on the observed data from 1967–1982, Reed (1986) concluded that the sub-Saharan baroclinic zone and near-equatorial rain belt jointly spawn about the same number of disturbances over Africa each year, but that fewer strong and/or highly convective disturbances occurred near the coast during periods of extended droughts, which was reproduced by the degraded experiments of Xue and Shukla (1993). However, some recent observational data from Niger (Le Barbé and Lebel 1997) shows that the drought in Niger was mostly associated with a decrease in the number of rain events in July and August. More studies with mesoscale and regional models are necessary to understand the relationship between individual rain events and land-surface conditions.

To summarize the impact of the land surface on the Sahel regional climate, the changes in albedo and/or initial soil moisture from different experiments are given in Table 4.2. The

Table 4.2 Comparison of different Sahel experiments.

Source	Location (°N)	Albedo Change	Initial Soil Moisture Change	Change in E mm day^{-1}	Change in P mm day^{-1}	% Change in P for 0.1 Albedo Change
Charney et al. (1977)	16–20	0.21		–0.9	–3.4	–22
Chervin & Schneider (1976)	N. of 8	0.22			–2.5	–18
Cunnington & Rowntree (1986)	N. of 10	0.07		–0.21	–0.25	–33
Kitoh et al. (1988)	0–12	0.13		–1.2	–2.1	–23
Kitoh et al. (1988)	0–12	0.13	–13.5 cm	–2.3	–2.7	–29
Laval & Picon (1986)	14–21	0.13		–0.5	–0.8	–18
Sud & Fennessy (1982)	12–20	0.12		–0.7	–1.5	–21
Xue et al. (1990)	10–20	0.08	–16 cm	–1.7	–1.5	
Xue & Chukla (1993)	10–19	0.10	–0.1 (wetness)	–0.7	–1.5	–22
Xue (1997)	10–19	0.10	–0.1 (wetness)	–0.8	–1.3	–30

corresponding change in precipitation is also given. Because the different GCMs predicted very different mean precipitation in the Sahel, the relative changes (%) of the precipitation are also given for comparison. Table 4.2 clearly demonstrates that despite the wide range of different surface models, ranging from very simple land-surface models to complex biophysical models, the results for the northern African studies are quite consistent: albedo (soil moisture) changes produce negative (positive) feedbacks. Even the magnitude of the impacts is within a close range, which supports the results from the experiments presented here.

EAST ASIAN DESERTIFICATION STUDY

The relationship between land-surface degradation in the Mongolian and Inner Mongolian grassland and the drought in East Asia has also been studied in numerical simulations. Because of high internal variability in this region in the real world and in model simulations, there are few studies investigating the interactions between land surface and atmosphere. Here we describe the results from an ensemble of six 3-month integrations with the coupled COLA GCM/SSIB model.

In the simulation experiments, the vegetation in the degraded area was changed from grassland (Type 7) to bare soil (Type 11, Figure 4.4, Table 4.1). The specification of the degraded area in this experiment was based on a desertification map compiled by Zhu et al. (1988). Three control integrations and three desertification integrations over the East Asian summer monsoon period (early June through August) were conducted using different initial atmospheric conditions. The results indicated that degradation of the grassland could have a substantial impact on the regional climate and on some important features of the East Asian summer monsoon.

Precipitation in China has generally decreased over the past forty years, particularly in southern China and northern China. A "sandwich pattern" has been observed: negative

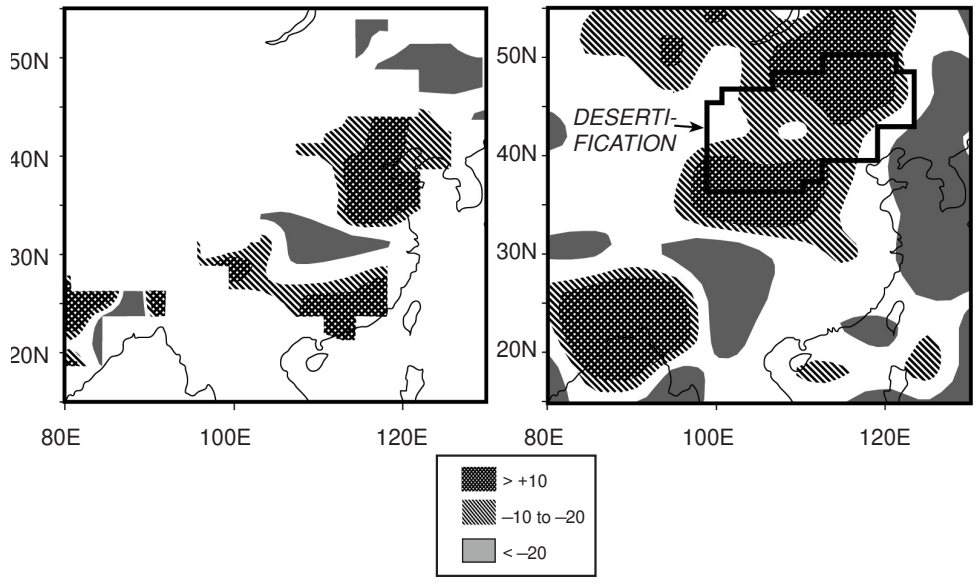

Figure 4.4 (a) Observed June-July-August (JJA) rainfall difference over East Asia between the 1980s and 1950s. (b) Ensemble mean JJA precipitation difference (degraded minus control simulations). Degraded area is enclosed by heavy line. Units are mm month^{-1}.

changes to the south and north of the Yangtze River and a positive change in between (N-P-N pattern). Figure 4.4 shows the observed June-July-August (JJA) rainfall difference between the 1980s and the 1950s, and the simulated rainfall differences between the desertification runs and the control runs. The observed N-P-N pattern is simulated, but the axis is tilted to the southwest of that observed. The rainfall reductions occur within the desertification area, but also to the south of the desertification area. The rainfall is reduced by 19.3 mm month^{-1}, (more than 10%) in the desertification experiments over the area with the maximum rainfall reduction (34°N to 48°N, and 100°E to 115°E).

The JJA surface air temperatures over the desertification area were higher in the desertification experiment, by 1.3°K. The temperature increase in the atmosphere occurred only at low atmospheric levels, below 850 mb. The upper atmosphere became cooler by about 0.5°C. Based on observations from 410 stations over China, Chen et al. (1994) found that the yearly mean surface air temperature increased over most of China during the past forty years, mainly during winter. In summer, much of China became cooler. However, over the Inner Mongolian grassland, the summer surface air temperature was warmer during the 1980s.

The simulated soil moisture and surface evaporation was substantially reduced in the desertification experiments over the desertification area, which was similar to that found in the Sahel desertification experiments. The increased surface albedo, reduced vegetation coverage, reduced soil water content, and reduced surface roughness resulted in reduced evaporation. Because of the reduction in precipitation, soil moisture also decreased. Surface runoff increased, however, due to the degradation in land-surface conditions, which again confirmed the results in the Sahel study, i.e., without the climate feedback fully in effect, the runoff increases due to the land degradation.

U.S. LAND-COVER CHANGE STUDY

Drought frequently occurs on the Great Plains area of the U.S. (Karl and Quayle 1981; Cook et al. 1999), with particularly notable events in the 1930s (Warrick 1980), 1950s (Namias 1955), and 1980s (Namias 1982). Land-cover changes due to human activity in the Great Plains region are apparent (Middleton 1999). Agricultural settlement of this semi-arid plain over the past century altered its floral, faunal, hydrological, and climatological conditions. The Dust Bowl of the 1930s in the Great Plains was one of the best-known drought environmental disasters in U.S. history. Although this event inspired major advances in soil conservation techniques, continued degradation is still an important issue in the Great Plains (Middleton 1999). We conducted a sensitivity study to investigate the impact of land-cover changes over the agricultural region in the central U.S. on North American regional climate.

In the numerical experiment, two land-cover conditions were assigned to the agricultural area over the Great Plains. In one simulation, the crop cover, LAI, and vegetation greenness over the U.S. Great Plains were specified close to satellite-observed values, with relatively high values of vegetation properties throughout JJA (e.g., LAI was about 6 and the green-leaf fraction about 0.9). In another simulation, field measurements at a single crop site after harvest were used to specify land conditions over the Great Plains. Since the vegetation cover and LAI were very low after harvest in the later simulation, there was an artificially created "degradation" in this simulation.

In an ensemble of three-month integrations from June to August, the simulated seasonal mean surface temperature was 2–4 K higher and the rainfall was 15–30 mm month^{-1} lower in these "degraded" integrations. Surface evaporation and soil moisture were also reduced. These impacts were very persistent throughout the three-month integrations. The degradation also influenced the temperature and humidity profiles in the lower troposphere.

Recently, mesoscale modelers have also conducted land–atmosphere interaction studies. These studies have shown (see, e.g., Pielke et al. 1999) that land-surface heterogeneity in the central U.S. could cause horizontal variations in the surface energy budget and generate mesoscale atmospheric circulations, which can focus precipitation and have a profound influence on the local weather.

UNDERSTANDING THE MECHANISMS

Simulated climate anomalies were caused by specified land degradation, which affected the atmosphere mainly through modulating the hydrological processes and energy balance at the surface. It is important to understand how these processes are altered as a result of land-cover changes. Because the surface albedo change caused by land degradation has a strong effect on the surface energy balance, it must be specified realistically. Despite the importance of albedo, changes in vegetation and soil properties (such as LAI) also contribute significantly to rainfall and surface temperature anomalies.

Because of the higher surface albedo, lower LAI, and higher stomatal resistance in the degradation simulations, evaporation was substantially lower in all three regions (Sahel, East Asia, and the Central U.S.), consistent with the simulated rainfall reductions. However, other components of the surface energy and water balance changed differently across the three regions. More shortwave radiation was reflected from the surface as a result of the higher

albedo, but this loss was partially compensated for by the increased incoming shortwave radiation, caused by less clouds in the drier atmosphere. In the southern Sahel, the cloud–radiation interaction was particularly strong, and the net shortwave radiation absorbed by the surface did not change.

Changes in the surface sensible heat flux were associated with the changes in shortwave radiation. The surface sensible heat flux was reduced when shortwave radiation decreases substantially (as in the northern Sahel, the Great Plains, and the East Asian regions). Otherwise, it increased to balance the reduction of latent heat flux in the surface energy budget (such as in the southern Sahel).

The net longwave radiation at the surface was reduced because the higher surface temperature increased the outgoing longwave radiation, and the reduced cloud and water vapor in the degradation simulations lowered the incoming longwave radiation at the surface. However, this reduction was less than that in surface latent heat flux.

Because of the large reduction in evaporation, less moisture was transferred to the atmosphere through the boundary layer. This resulted in less convection and lower atmospheric latent heating rates. The lower convective latent heating rate was responsible for more than 70% of the reduction in the total atmospheric diabatic heating rate in these experiments. The reduced total diabatic-heating rate in the atmosphere was associated with relative subsidence, less moisture flux convergence (MFC), and lower rainfall. These changes further reduced the evaporation and convective heating, producing a positive feedback.

The southwest monsoon flows from the Bay of Bengal and the Atlantic Ocean are the main summer moisture sources for East Asia and the Sahel, respectively. Studies of both regions showed that the land–atmosphere interaction resulting from land degradation weakened the monsoon flow and affected the atmospheric circulation and horizontal MFC. The area influenced by the land changes extended considerably beyond the area where the degradation was specified.

The changes in the MFC varied among the regions because they each have different large-scale circulations and moisture sources. The MFC was decreased in the Sahel study, consistent with the reduced convective heating. In both the East Asian and U.S. studies, the warmer surface induced more MFC, but this increase was much smaller than the reduction in surface evaporation. In all these regions changes in evaporation produced the most important impact on the regional hydrological balance (Table 4.3).

CONCLUSION

The results presented here show that land-cover changes are important aspects of the observed climate anomalies in East Asia and the Sahel. Because of the potentially devastating social and economic consequences of drought-induced famines in these regions, there has been a great deal of scientific interest in the causes of the current droughts. There are different views on the causes of the droughts. One states that the main cause is land-surface degradation as a result of population pressure in excess of the region's carrying capacity. Another view attributes the droughts to unfavorable anomalous patterns in sea-surface temperature. In both cases, the development of mitigation and adaptation strategies is needed to make these regions less vulnerable. Furthermore, it is also recognized that poor policies may also exacerbate drought situations (Watts 1983).

Table 4.3 Simulated ensemble mean differences between control and degradation experiments over different regions (mm month^{-1}).

Region*	South Sahel (JAS)	North Sahel (JAS)	East Asia (JJA)	Central U.S. (JJA)
Precipitation	–56	–29	–17	–13.5
Evaporation	–26	–21	–21	–27
Moisture flux convergence	–29	–12	3	12

* South Sahel, from 9°N to 13°N and 15°W to 43°E; North Sahel, from 13°N to 17°N and 15°W to 43°E; East Asia, from 39°N to 48°N and 100°E to 120°E; Central U.S., from 30° to 45°N and 90° to 105°W.

JAS: July-August-September mean JJA: June-July-August mean

Studies of the Sahel have been going on for more than two decades. Scientific results have consistently demonstrated that land-cover degradation has had significant impacts on the regional climate. Early modeling studies were mainly sensitivity studies. When coupled atmosphere–biosphere models were introduced for land degradation–atmosphere interaction studies, the results revealed that numerical experiments not only tested the sensitivity of the regional climate to land-surface processes, but were also able to link the land-surface processes to observed decadal climate anomalies.

In particular, when a coupled model was used, both the summer and fall anomalies observed over the African continent and the summer drought patterns in East Asia were simulated in the land degradation experiments. This indicates that the coupled climate–biosphere model may be able to provide an assessment of the potential consequences of human activities and predict the regional climate changes resulting from land degradation. More model validation and comparisons are necessary before these models can be used for these applications.

The East Asia simulations reviewed in this chapter are the first to link land degradation and decadal drought in the area. The U.S. study revealed the possible consequences of land degradation in the U.S. Great Plains, which is consistent with what happened during the dust storm of the 1930s. More research, however, is necessary to understand further the impact and mechanisms in these two regions. By comparing studies over different regions of the world we gain more insight into the physical mechanisms of land surface–atmosphere interactions and their role in regional climate change.

In both the East Asian and Great Plains simulation studies, land-surface conditions were specified. Vegetation conditions did not vary with the climate conditions. Most recently, an additional level of complexity is being explored by the coupling of dynamic vegetation models to atmospheric models. Though still in its early development, this field has already produced a number of interesting results regarding land surface–climate interactions in the Sahel (see, e.g., Claussen 1998; Wang and Eltahir 2000). With the development of dynamic vegetation models, we may be able to assess more realistically the role of sea surface temperatures, land-surface processes, and other processes in long-term Sahel drought.

Since desertification usually happens in patches (Goudie 2000), the specification of uniform degradation in the previous experiments did not represent the real desertification situation and might exaggerate the impact of the land degradation. Regional or mesoscale models

embedded within GCMs are necessary to assess more realistically the consequences of desertification in local scales, especially the effect of spatial heterogeneity. They will not only help in specifying the land degradation conditions but also in the transfer of the information from large-scale global models to regional or local scales.

In the numerical experiments described herein, the specifications of land degradation are crucial. It is still unclear how well the normal and degraded vegetation scenarios specified in the Sahel and East Asian studies represent the real land-surface conditions in the 1950s and 1980s. Research is underway to use population information to produce more realistic reconstructions of land-surface dynamics over the past forty years and to make projections for the future (Stephenne and Lambin 2001). In addition, cesium 137 techniques hold promise in being able to provide soil loss information (Chappell et al. 1998), and satellite data will provide additional information regarding land degradation (see Prince 2002).

In summary, if the changes in vegetation properties that occurred between the 1950s and 1980s are comparable to the specified control/desertification differences, our results indicate that anthropogenic land degradation could lead to regional climate changes similar to those previously observed. To avoid such consequences, the implementation of sustainable resource management policies must be a priority. Another numerical study (Xue and Shukla 1996) demonstrated that afforestation of the Sahel might reverse the regional climate changes caused by land degradation. Although this kind of large-scale experiment might be unrealistic in the real world, due to political and economical constraints and the potential consequence of the competitive equilibrium between herbaceous and woody plants, many places have conducted land improvement programs. Some agricultural practices which utilize an anti-crisis narrative have been explored (e.g., Leach and Mearns 1996). As more information from these land improvement programs becomes available, we should be able to assess realistically their influence on the regional climate.

ACKNOWLEDGMENT

We wish to thank M. Hulme (University of East Anglia, Norwich) for meteorological data. Funding was provided by NSF grants EAR–0096203 and NASA grants NAG5–9014.

REFERENCES

Chappell, A., A. Warren, M.A. Oliver, and M. Charlton. 1998. The utility of 137Cs for measuring soil redistribution rates in south-west Niger. *Geoderma* **81:**313–338.

Charney, J.G. 1975. Dynamics of deserts and drought in the Sahel. *Qtly. J. Roy. Meteor. Soc.* **101:**193–202.

Charney, J.G., W.K. Quirk, S.-H. Chow, and J. Kornfield. 1977. A comparative study of the effects of albedo change on drought in semi-arid regions. *J. Atmos. Sci*. **34:**1366–1385.

Chen, L., Y. Shao, and Z. Ren. 1994. Climate change in China during the past 70 years and its relationship to the variation of monsoon. In: Climate–Biosphere Interactions: Biogenic Emissions and Environmental Effects of Climate Change, ed. R.G. Zepp, pp. 31–50. New York: Wiley.

Chervin, R.M., and S.H. Schneider. 1976. On determining the statistical significance of climate experiments with general circulation models. *J. Atmos. Sci.* **33:**405–412.

Clark, D., Y. Xue, P. Valdes, and R. Harding. 2001. Impact of land surface degradation over different subregions in Sahel on climate in tropical North Africa. *J. Climate* **14**:1809–1822.

Claussen, M. 1998. On multiple solutions of the atmosphere-vegetation system in present-day climate. *Glob. Change Biol.* **4**:549–559.

Cook, E.R., D.M. Meko, D.W. Stable and M.K. Cleaveland. 1999. Drought reconstruction for the continental United States. *J. Climate* **12:**1145–1161.

Cunnington, W.M., and P.R. Rowntree. 1986. Simulations of the Saharan atmosphere-dependence on moisture and albedo. *Qtly. J. Roy. Meteor. Soc.* **112:**971–999.

Dickinson, R.E., A. Henderson-Sellers, P.J. Kennedy, and M.F. Wilson. 1986. Biosphere-atmosphere schemes (BATS) for the NCAR community climate model. NCAR Technical Notes NCAR/TN-275+STR. Boulder, CO: National Center for Atmospheric Research.

Dregne, H.E., and N.T. Chou. 1992. Global desertification dimensions and costs. In: Degradation and Restoration of Arid Lands, ed. H.E. Dregne, pp. 249–282. Lubbock, TX: Texas Tech Univ.

Gornitz, V. 1985. A survey of anthropogenic vegetation changes in West Africa during the last century — Climate implication. *Clim. Change* **7**:285–235.

Goudie, A. 2000. The Human Impact in the Natural Environment. Cambridge, MA: MIT Press.

Hulme, M. 1992. A 1951–80 global land precipitation climatology for the evaluation of General Circulation Models. *Clim. Dyn.* **7:**57–72.

Karl, T.B., and R.G. Quayle. 1981. The 1980 summer heat wave and drought in historical perspective. *Mon. Wea. Rev.* **109**:2055–2073.

Kinter, J.L., III, J. Shukla, L. Marx, and E.K. Schneider. 1988. A simulation of the winter and summer circulation with the NMC global spectral model. *J. Atmos. Sci*. **45:**2486–2522.

Kitoh, A., K. Yamazaki, and T. Tokioka. 1988. Influence of soil moisture and surface albedo changes over the African tropical rain forest on summer climate investigated with the MRI-GCM-I. *J. Meteor. Soc*. *Japan* **66:**65–85.

Laval, K., and L. Picon. 1986. Effect of a change of the surface albedo of the Sahel on climate. *J. Atmos. Sci.* **43:**2418–2429.

Leach, M., and R. Mearns. 1996. The Lie of the Land: Challenging Received Wisdom on the African Environment. Oxford: Intl. African Institute.

Le Barbé, L., and T. Lebel 1997. Rainfall climatology of the HAPEX-Sahel region during the years 1960–1990. *J. Hydrol.* **188–189**:43–73.

Middleton, N. 1999. The Global Casino: An Introduction to Environmental Issues. New York: Oxford Univ. Press.

Namias, J. 1955. Some meteorological aspects of drought with special reference to the summers of 1952–54 over the United States. *Mon. Wea. Rev.* **83:**199–205.

Namias, J. 1982. Anatomy of Great Plains protracted heat waves (especially the 1980 U.S. summer drought). *Mon. Wea. Rev.* **110:**824–838.

Nicholson, S.E. 2002. What are the key components of climate as a driver of desertification? In: Global Desertification: Do Humans Cause Deserts?, ed. J.F. Reynolds and D.M. Stafford Smith, pp. 41–57. Dahlem Workshop Report 88. Berlin: Dahlem Univ. Press.

Nicholson, S.E., C.J. Tucker, and M.B. Ba. 1998. Desertification, drought, and surface vegetation: An example from the West African Sahel. *Bull. Am. Meteorol. Soc*. **79**:815–829.

Norton, C.C., F.R. Mosher, and B. Hinton. 1979. An investigation of surface albedo variations during the recent Sahel drought. *J. Appl. Meteor.* **18:**1252–1262.

Pielke, R.A., R. Avissar, M. Raupach et al. 1999. Interactions between the atmosphere and terrestrial ecosystems: Influence on weather and climate. *Glob. Change Biol.* **4:**461–475**.**

Prince, S.D. 2002. Spatial and temporal scales for detection of desertification. In: Global Desertification: Do Humans Cause Deserts?, ed. J.F. Reynolds and D.M. Stafford Smith, pp. 23–40. Dahlem Workshop Report 88. Berlin: Dahlem Univ. Press.

Reed, R.J. 1986. On understanding the meteorological causes of Sahelian drought. In: Persistent Meteo-oceanographic Anomalies and Teleconnections, ed. C. Chagas and G. Puppi, pp. 179–213. Vatican City: Pontificia Academia Scientiarum, Ex Aedibus Academicis.

Stephenne, N., and E.F. Lambin. 2001. A dynamic simulation model of land-use changes in the African Sahel (SALU). *Agr. Ecosys. Env.* **85:**145–162.

Sud, Y.C., and M. Fennessy. 1982. A study of the influence of surface albedo on July circulation in semiarid regions using the GLAS GCM. *J. Climatol*. **2:**105–125.

Sud, Y.C., and M. Fennessy. 1984. A numerical study of the influence of evaporation in semiarid regions on the July circulation. *J. Climatol.* **4**:383–398.

Sud, Y.C., and A. Molod. 1988. A GCM simulation study of the influence of Saharan Evapotranspiration and surface-albedo anomalies on July circulation and rainfall. *Mon. Wea. Rev*. **116:**2388–2400.

UNEP (United Nations Environment Programme). 1992. World Atlas of Desertification. Editorial commentary by N. Middleton and D.S.G. Thomas. London: Edward Arnold.

Walker, J., and P.R. Rowntree. 1977. The effect of soil moisture on circulation and rainfall in a tropical model. *Qtly. J. Roy. Meteor. Soc*. **103:**29–46.

Wang, G., and E.A.B. Eltahir. 2000. Role of vegetation dynamics in enhancing the low-frequency variability of the Sahel rainfall. *Water Resources Res.* **36:**1013–1021.

Warrick, R.A. 1980. Drought in the Great Plains: A case study of research on climate and society in the U.S.A. In: Climatic Constraints and Human Activities, ed. J. Ausubel and A.K. Biswas, pp. 93–124. Oxford: Pergamon.

Watts, M. 1983. Silent Violence: Food, Famine, and Peasantry in Northern Nigeria. Berkeley: Univ. of California Press.

WRI (World Resource Institute). 1994. World Resources 1994–1995. New York: Oxford Univ. Press.

Xue, Y. 1996. The impact of desertification in the Mongolian and the Inner Mongolian grassland on the regional climate. *J. Climate* **9:**2173–2189.

Xue, Y. 1997. Biosphere feedback on regional climate in tropical North Africa. *Qtly. J. Roy. Meteor. Soc.* **123**:B:1483–1515.

Xue, Y., D.B. Clark, T. Oki, and R.J. Harding. 2000. Biosphere feedback on rainfall, surface temperature, and runoff in West Africa. In: Proc. of the Workshop on the West African Monsoon Variability and Predictability, pp. 39–42. Tropical Meteorology Research Programme (TMRP) 63. World Meteorological Organization, Technical Documents WMO/TD 1003. Geneva: WMO.

Xue, Y., M.J. Fennessy, and P.J. Sellers. 1996. Impact of vegetation properties on U.S. summer weather prediction. *J. Geophys. Res*. **101**(**D3**):7419–7430.

Xue, Y., R.W.A. Hutjes, R.J. Harding et al. 2000. The Sahelian climate. In: Biospheric Feedback in the Climate System and the Hydrological Cycle, ed. P. Kabat, M. Claussen et al., chap. 4. Heidelberg: Springer, in press.

Xue, Y., K.-N. Liou, and A. Kasahara. 1990. Investigation of the biophysical feedback on the African climate using a two-dimensional model. *J. Climate* **3:**337–352.

Xue, Y., P.J. Sellers, J.L. Kinter III, and J. Shukla. 1991. A simplified biosphere model for global climate studies. *J. Climate* **4:**345–364.

Xue, Y., and J. Shukla. 1993. The influence of land surface properties on Sahel climate. I. Desertification. *J. Climate* **6:**2232–2245.

Xue, Y., and J. Shukla. 1996. The influence of land surface properties on Sahel climate. II. Afforestation. *J. Climate* **9**:3260–3275.

Yatagai, A., and T. Yasunari. 1995. Interannual variations of summer precipitation in the arid/semi-arid region in China and Mongolia. *J. Meteor. Soc. Japan* **73:**909–923.

Zhu, Z., S. Liu, and X. Di. 1988. Desertification and Rehabilitation in China. Peking: Academic.